Ruffling in a Series of Nickel(II) meso-Tetrasubstituted Porphyrins as a Model for the Conserved Ruffling of the Heme of Cytochromes c

ARTICLE *in* JOURNAL OF THE AMERICAN CHEMICAL SOCIETY · NOVEMBER 1995

Impact Factor: 12.11 · DOI: 10.1021/ja00150a008

Ruffling in a Series of Nickel(II) *meso*-Tetrasubstituted Porphyrins as a Model for the Conserved Ruffling of the Heme of Cytochromes *c*

W. Jentzen,[†] M. C. Simpson,[†] J. D. Hobbs,[†] X. Song,[†,‡] T. Ema,[§] N. Y. Nelson,[§] C. J. Medforth,[§] K. M. Smith,[§] M. Veyrat,[∥] M. Mazzanti,[∥] R. Ramasseul,[∥] J.-C. Marchon,[∥] T. Takeuchi,[⊥] W. A. Goddard, III,[⊥] and J. A. Shelnutt*[,†,‡]

Contribution from the Fuel Science Department, Sandia National Laboratories, Albuquerque, New Mexico 87185-0710, Department of Chemistry, University of New Mexico, Albuquerque, New Mexico 87131, Department of Chemistry, University of California, Davis, California 95616, CEA/Département de Recherche Fondamentale sur la Matière Condensée/SESAM, Laboratoire de Chimie de Coordination, Centre d'Etudes Nucléaires de Grenoble, 38054 Grenoble, France, and Materials and Process Simulation Center, Beckman Institute, California Institute of Technology, Pasadena, California 91125

Received April 4, 1995[⊗]

Abstract: Metalloporphyrins undergo remarkable nonplanar distortions of the macrocycle that perturb the chemical and photochemical properties of these important protein cofactors. Further, the tertiary structure of the surrounding protein can manipulate these distortions as a means of regulating biological function. For cytochromes *c*, for example, an energetically unfavorable, conserved nonplanar distortion of the heme exists and likely plays a role in its electron-transfer function. The heme distortion is primarily of the ruffling (*ruf*) type (corresponding to the lowest frequency B_{1u}-symmetry normal mode) in which the pyrroles are twisted about the metal−$N_{pyrrole}$ bond. This B_{1u}-symmetry nonplanar distortion is commonly observed in metalloporphyrin crystal structures, as are the saddling (*sad*) B_{2u}-symmetry distortion, waving (*wav*) E_g-symmetry distortions, and doming (*dom*) A_{2u}-symmetry distortion. Each of these nonplanar distortions is expected to result in unique alterations of the chemical and physical properties of the nominally planar porphyrin macrocycle. Symmetrical porphyrin substitution with tetrahedrally bonded atoms at the four *meso* bridging carbons generally results in the B_{1u} ruffling distortion; therefore, we investigated a series of *meso*-tetrasubstituted porphyrins for which the substituents vary in size (methyl, ethyl, propyl, pentyl, isopropyl, cyclopropyl derivative **11a**, cyclohexyl, apopinenyl (**10**), *tert*-butyl, adamantyl), increasing the steric crowding at the periphery. Molecular mechanics calculations show increasing degree of ruffling ($C_\alpha NNC_\alpha$ angle for opposite pyrroles varies from 0 to 57°) for this series of porphyrins, generally agreeing with the X-ray structures that are available. In addition, the frequencies of the structure-sensitive Raman lines decrease nonlinearly with increasing ruffling angle. The localization of the B_{1u} nonplanar distortion in only the $C_\alpha-C_m$ bond torsion (not the case for the B_{2u} *sad* distortion) suggests a means by which the B_{1u} distortion might be distinguished from other types of nonplanar distortion by using resonance Raman spectroscopy. Also, the size of the red shifts in the $\pi \rightarrow \pi^*$ absorption bands depends on $C_\alpha-C_m$ torsion angle in a nonlinear fashion and the shift is accurately predicted by INDO/s molecular orbital calculations when the nonplanar structures obtained from molecular mechanics are used.

Introduction

Recently, we noticed that all of the high-resolution X-ray crystal structures of cytochromes *c* show an iron porphyrin cofactor that is distorted from planarity by a significant degree.[1a] This heme distortion, primarily consisting of the ruffling (*ruf*) distortion as classified by Scheidt and Lee,[2] is highly conserved for mitochondrial cytochromes *c* from diverse species and also for other *c*-type cytochromes such as turnip cytochrome *f*.[1b] Furthermore, a secondary asymmetrical nonplanar distortion is superimposed on this ruffling and it is also conserved.[1a] Specifically, the pyrroles that possess covalent linkages to the protein backbone of cytochrome *c* are observed to be more distorted from the mean heme plane than the other two pyrroles. We[3-5] and others[6-8] have shown that nonplanar distortions of metalloporphyrins can significantly alter chemical and photo-

[†] Sandia National Laboratories.
[‡] University of New Mexico.
[§] University of California, Davis.
[∥] Centre d'Etudes Nucléaires de Grenoble.
[⊥] California Institute of Technology.
[⊗] Abstract published in *Advance ACS Abstracts,* November 1, 1995.

(1) (a) Hobbs, J. D.; Shelnutt, J. A. *J. Protein Chem.* **1995**, *14*, 19. (b) Martinez, S. E.; Smith, J. L.; Huang, D.; Szczepaniak, A.; Cramer, W. A. In *Research in Photosynthesis*; Murata, N., Ed.; Proceedings of the IXth International Congress on Photosynthesis; Kluwer Academic: Dordrecht, The Netherlands, 1992; Vol. 2, p 495.
(2) Scheidt, W. R.; Lee, Y. J. *Struct. Bonding (Berlin)* **1987**, *64*, 1.
(3) Alden, R. G.; Ondrias, M. R.; Shelnutt, J. A. *J. Am. Chem. Soc.* **1990**, *112*, 691.
(4) Hobbs, J. D.; Majumder, S. A.; Luo, L.; Sickelsmith, G. A.; Quirke, J. M. E.; Medforth, C. J.; Smith, K. M.; Shelnutt, J. A. *J. Am. Chem. Soc.* **1994**, *116*, 3261.
(5) Sparks, L. D.; Medforth, C. J.; Park, M.-S.; Chamberlain, J. R.; Ondrias, M. R.; Senge, M. O.; Smith, K. M.; Shelnutt, J. A. *J. Am. Chem. Soc.* **1993**, *115*, 581.
(6) (a) Barkigia, K. M.; Chantranupong, L.; Smith, K. M.; Fajer, J. *J. Am. Chem. Soc.* **1988**, *110*, 7566. (b) Fajer, J. *Chem. Ind. (London)* **1991**, 869.
(7) (a) Kratky, C.; Waditschatka, R.; Angst, C.; Johansen, J.; Plaquevent, J. C.; Schreiber, J.; Eschenmoser, A. *Helv. Chim. Acta* **1982**, *68*, 1312. (b) Waditschatka, R.; Kratky, C.; Jaun, B.; Heinzer, J.; Eschenmoser, A. *J. Chem. Soc., Chem. Commun.* **1985**, 1604.
(8) (a) Kadish, K. M.; Caemelbecke, E. V.; D'Souza, F. D.; Medforth, C. J.; Smith, K. M.; Tabard, A. *Organometallics* **1993**, *12*, 2411. (b) Kadish, K. M.; Caemelbecke, E. V.; Boulas, P.; D'Souza, F. D.; Vogel, E.; Kisters, M.; Medforth, C. J.; Smith, K. M. *Inorg. Chem.* **1993**, *32*, 4177.

0002-7863/95/1517-11085$09.00/0

physical properties of metalloporphyrins. Of particular importance for an electron-transport protein like cytochrome *c* is the modification of the oxidation−reduction properties of the heme by nonplanar distortion.[5-8] Specifically, protein-controlled ruffling of the heme provides a mechanism by which the tertiary structure of the surrounding protein can regulate heme reduction potentials.

In another recent study, we demonstrated that naturally-occurring iron porphyrins are expected to be planar in the absence of external perturbations.[9] This is not the case for porphyrins containing metals like Ni(II) that favor a significantly shorter metal−nitrogen distance than the optimum distance favored by the porphyrin macrocycle (ca. 2.00 Å).[10] In order to determine the magnitude of the external perturbation required to cause a nonplanar distortion, we investigated[4,5,11,12] several series of highly substituted synthetic porphyrins for which the external perturbation is supplied by steric crowding of the peripheral substituents. In particular, we demonstrated that sizable steric interactions at the periphery are necessary to cause nonplanar distortions of porphyrins if the metal ions are as large as Cu(II) and Fe(III).[9] Thus, the nonplanar distortion of the heme of cytochrome *c* is likely the result of forces exerted by (1) the covalent linkages between the heme and the protein backbone, (2) the hydrogen bonds between the propionic acid substituents of the heme and amino acids of the protein, (3) the interactions with the axial ligands, and (4) the steric interactions with protein side chains in contact with the heme.

In most previous studies,[4-6,11,12] the type of nonplanar distortion is either unknown or of the *sad* type distortion rather than the *ruf* type. Therefore, a good model system for which the distortion is known to be of the *ruf* classification is needed so that the effects of ruffling on the heme can be determined and differentiated from the effects of other types of nonplanar distortion. Also, such a model system would be generally useful for developing spectroscopic methods suitable for distinguishing various types of nonplanar distortions of metalloporphyrins.

Herein, we explore the structural and spectroscopic properties of a series of nickel(II) *meso*-tetrasubstituted porphyrins, Ni-**1** to Ni-**11a**, shown in Figure 1. The substituents are mostly alkyl groups of varying size including methyl (TMeP, **1**), ethyl (TEtP, **2**), propyl (TPrP, **3**), pentyl (TPeP, **4**), isopropyl (TiPrP, **5**), cyclohexyl (TcHP, **6**), *tert*-butyl (TtBuP, **7**), and adamantyl (TAdP, **8**) groups. For comparison purposes the tetrasubstituted porphyrins with phenyl (TPP, **9**), apopinenyl (TMyP, **10**), and a cyclopropyl (TcPrP, **11**) derivative (TcPrP-**11a**, **11a**) are also included in the series. We have calculated the conformations of these Ni porphyrins using a molecular mechanics force field similar to one used previously by us to predict structures of metalloporphyrins.[1a,4,5,9,11,12] As expected, all of the porphyrins are found to be ruffled rather than in other nonplanar conformations (see Figure 2). X-ray crystal structures of some of these porphyrins have been reported, and the calculated structures are generally consistent with the X-ray crystallographic results. Structural parameters obtained from the calculated conformations are correlated with spectroscopic data, including frequencies of structure-sensitive Raman lines and wavelengths of the optical absorption bands of the porphyrin. A structural explanation for the Raman frequency shifts due to ruffling is proposed. A structural interpretation of the frequency shifts is possible for this series because the electronic inductive properties of the alkyl substituents are all approximately the same (σ_m is −0.7 for the methyl, ethyl, and isopropyl groups and −0.10 for *tert*-butyl),[12e] allowing us to neglect electronic effects on the spectra. INDO/s molecular orbital calculations for these nickel porphyrins show that the UV−visible band shifts are primarily a result of conformational differences rather than electronic differences in the substituents.

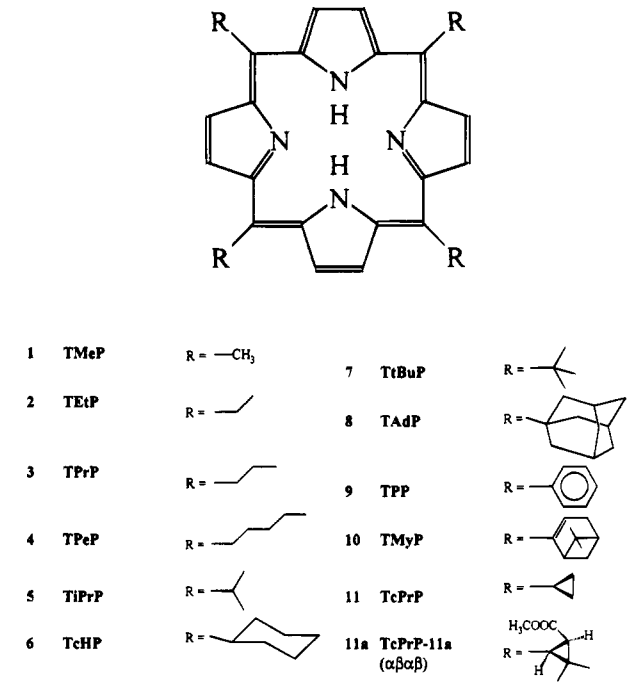

Figure 1. Nickel(II) *meso*-tetrasubstituted porphyrins. Substituent R groups are indicated.

Materials and Methods

Syntheses. Porphyrins H_2TMeP (**1**), H_2TEtP (**2**), and H_2TPeP (**4**) were prepared using a published procedure.[13] Porphyrins H_2TiPrP (**5**) and H_2TtBuP (**7**) were prepared using a modified version of this procedure in which the concentration of the pyrrole and the aldehyde was increased to 150 mM and the concentration of the BF_3·OEt_2 catalyst was increased to 25 mM.[14] H_2TAdP (**8**) was synthesized from 1-adamantanemethanal and pyrrole using the procedure described for porphyrins **5** and **7**. To prepare 1-adamantanemethanal, a 1000-mL round-bottomed flask was equipped with a magnetic stirrer and nitrogen inlet, and dry dichloromethane (300 mL), 4-Å molecular sieves, 1-adamantanemethanol (2.00 g), and 4-methylmorpholine *N*-oxide (4.25 g) were added. The solution was stirred for 15 min under a nitrogen atmosphere, tetrapropylammonium perruthenate(VII) (0.197 g) was added, and the solution was stirred for an additional 1 h. The molecular sieves and any solid material were removed by filtration, whereupon the filtrate was diluted with dichloromethane (600 mL), washed with water (2 × 1000 mL) and saturated sodium chloride (2 × 500 mL), and dried over anhydrous sodium sulfate. The solution was concentrated and columned using silica gel with dichloromethane as the eluent. The aldehyde portion was collected, and the solvent was then removed under vacuum to give 1-adamantanemethanal as a white solid in 83% yield. This compound was used without further purification in the preparation of H_2TAdP (**8**). To purify H_2TAdP (**8**), any solid polymeric

(9) Anderson, K. K.; Hobbs, J. D.; Luo, L.; Stanley, K. D.; Quirke, J. M. E.; Shelnutt, J. A. *J. Am. Chem. Soc.* **1993**, *115*, 12346.
(10) Hoard, J. L. *Ann. N.Y. Acad. Sci.* **1973**, *206*, 18.
(11) Shelnutt, J. A.; Medforth, C. J.; Berber, M. D.; Barkigia, K. M.; Smith, K. M. *J. Am. Chem. Soc.* **1991**, *113*, 4077.
(12) (a) Medforth, C. J.; Berber, M. D.; Smith, K. M.; Shelnutt, J. A. *Tetrahedron Lett.* **1990**, *31*, 3719. (b) Medforth, C. J.; Senge, M. O.; Smith, K. M.; Sparks, L. D.; Shelnutt, J. A. *J. Am. Chem. Soc.* **1992**, *114*, 9859. (c) Shelnutt, J. A.; Majumder, S. A.; Sparks, L. D.; Hobbs, J. D.; Medforth, C. J.; Senge, M. O.; Smith, K. M.; Miura, M.; Luo, L.; Quirke, J. M. E. *J. Raman Spectrosc.* **1992**, *23*, 523. (d) Miura, M.; Majumder, S. A.; Hobbs, J. D.; Renner, M. W.; Furenlid, L. R.; Shelnutt, J. A. *Inorg. Chem.* **1994**, *33*, 6078. (e) Hansch, C.; Leo, A. *Substituent Constants for Correlation Analysis in Chemistry and Biology*; J. Wiley & Sons: New York, 1979; Chapter 6.
(13) Lindsey, J. S.; Schreiman, I. C.; Hsu, H. C.; Kearney, P. C.; Marguerettaz, A. M. *J. Org. Chem.* **1987**, *52*, 827.
(14) Ema, T.; Senge, M. O.; Nelson, N. Y.; Ogoshi, H.; Smith, K. M. *Angew. Chem., Int. Ed. Engl.* **1994**, *33*, 1879.

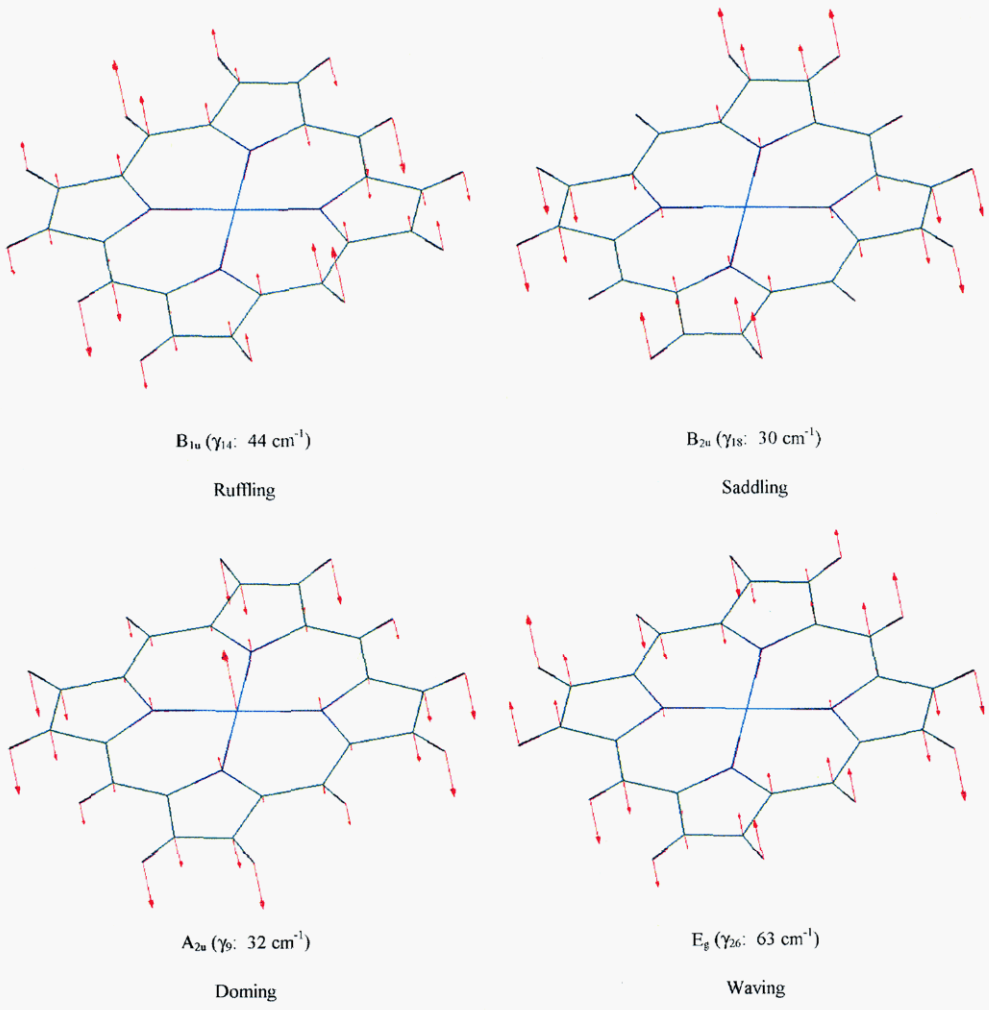

Figure 2. Atomic displacements in the lowest frequency normal modes of B_{1u}, B_{2u}, A_{u2}, and E_g (x) symmetries for nickel porphine. The naming convention and frequencies are from the normal coordinate analysis for nickel octaethylporphyrin.[23a]

materials formed during the reaction were filtered off, the filtrate was diluted to a 6-fold volume with dichloromethane, and the solution was passed through a short column of Grade III Alumina to remove any baseline impurities. The solvent was then removed under vacuum and the crude product recrystallized from dichloromethane by addition of *n*-hexane. H_2TAdP (**8**) was obtained in 6.3% yield. Nickel was inserted using the acetate method,[15] and the nickel porphyrins were purified by recrystallization from dichloromethane by addition of methanol.

H_2TcHP (**6**),[16,17] H_2TMyP (**10**),[18] and $\alpha\beta\alpha\beta$-H_2TcPrP (**11a**)[18] were also prepared by the Lindsey method[13] in 23%, 11%, and 4% yields, respectively, from pyrrole and the corresponding aldehyde (cyclohexanecarboxaldehyde (Aldrich), (1*R*)-(−)-myrtenal (Aldrich), and (1*R*)-*cis*-caronaldehydic methyl ester[19]). These nickel(II) derivatives were also prepared using the metal acetate method and were purified by column chromatography on silica gel with 1:1 dichloromethane−hexane as the eluent. The complexes were recrystallized from chloroform−acetonitrile. A sample of NiTPrP (Ni**3**) was kindly provided by J. Fajer. NiTPP (Ni-**9**) was obtained from Porphyrin Products, Inc.

Spectroscopy. Resonance Raman spectra were obtained using a dual-channel spectrometer described previously.[20] The solution spectra of porphyrin samples and reference compounds (usually NiTPP) were obtained simultaneously in separate compartments of a cylindrical rotating quartz cell. Rotation of the Raman cell at 50 Hz prevented local heating of the sample even with incident laser powers as high as 100 mW. In some cases spectra of the solid powders were also obtained. Krypton (Coherent, INNOVA 20) and argon (Coherent, INNOVA 20) ion lasers provided excitation wavelengths in the Soret and β band regions of the absorption spectrum. The scattered light was collected in a 90° scattering geometry. Polarized spectra were measured by passing the scattered light through a Polaroid sheet oriented parallel or perpendicularly to the scattered plane followed by a scrambler in front of the spectrometer entrance slit. The spectral slit widths of the spectrometer were in the range 2−6 cm^{-1}.

For solution spectra, the metalloporphyrins were dissolved in carbon disulfide and were added to each side of a two-compartment Raman cell. The sample and reference concentrations were about 0.1 mM in solvents of spectroscopic grade (Aldrich). Spectra of the polycrystalline samples (powder spectra) were obtained by using the spectrometer in the conventional single-channel mode. Sample integrity was monitored with UV−visible absorption spectroscopy. No sample decomposition was noted in the absorption spectra or successive Raman scans of the spectral region.

The spectra shown are the unsmoothed sum of several scans. The typical experimental conditions were 40-mW laser power for the solution spectra and 20-mW (defocused) for the polycrystalline spectra, 5-cm^{-1} spectral slit width, three scans with 0.4-cm^{-1} increment, and 1-s integration time. The frequency calibration of the solution spectra in the regions above and below 900 cm^{-1} was carried out by using the 1373.3- and 391.9-cm^{-1} lines of NiTPP in carbon disulfide, respectively; a NiTPP solution was added to the reference chamber for this purpose. The spectra of NiTPP were calibrated with the 992.0-cm^{-1} line of benzene.[21] The frequency calibration of the powder spectra was carried

(15) Buchler, J. W. In *Porphyrins and Metalloporphyrins*; Smith, K. M., Ed.; Elsevier: Amsterdam, 1975; Chapter 5, p 179.
(16) Onaka, M.; Shinoda, T.; Izumi, Y.; Nolen, E. *Chem. Lett.* **1993**, 117.
(17) Veyrat, M.; Ramasseul, R.; Marchon, J.-C.; Turowska-Tyrk, I.; Scheidt, W. R. *New J. Chem.* **1995**, in press.
(18) Veyrat, M.; Maury, O.; Faverjon, F.; Over, D. E.; Ramasseul, R.; Marchon, J.-C.; Turowska-Tyrk, I.; Scheidt, W. R. *Angew. Chem., Int. Ed. Engl.* **1994**, *33*, 220.
(19) Bakshi, D.; Mahidroo, V. K.; Soman, R.; Dev, S. *Tetrahedron* **1989**, *45*, 767.
(20) Shelnutt, J. A. *J. Phys. Chem.* **1983**, *87*, 605.

out by using standard pencil lamps (Ar, Kr) which were calibrated with the 992.0-cm^{-1} line of benzene as well. Additionally, all spectra were corrected for nonlinearity of the spectrometer to obtain the absolute frequency position of the lines. The peak positions and full line widths of the Raman lines were obtained by decomposing the Raman spectra into Lorentzian lines convoluted with a triangular slit function.[22] The nonlinear least-squares curve fitting was carried out with the program PeakFit (Jandel Scientific). The reproducibility of the spectra was checked by running the spectra several times. The standard deviation in the absolute frequency reading was ± 0.6 cm^{-1}.

The near UV and visible spectra were obtained with a 10-mm quartz cell using a Hewlett-Packard HP 8452A diode array spectrophotometer. The absorption spectra of the porphyrins were taken in carbon disulfide. The peak positions of the absorption bands were obtained by fitting the absorption spectra with Lorentzian or Gaussian lines. The estimated error in the relative band positions is ± 1 nm.

Molecular Modeling. Classical molecular mechanics calculations employed a force field based on recent normal coordinate analyses[23] of nickel porphyrins and the DREIDING II force field.[24] In the earlier version of the force field,[5,11] force constants for the bond stretches, bond angle bends, bond torsions, and inversions of the porphyrin macrocycle were taken to be the same as given by the normal coordinate analyses of NiOEP. Then, the unconstrained equilibrium bond length for the nickel–nitrogen(pyrrole) bond was set to 1.855 Å, and the other equilibrium bond distances were adjusted so that the energy-minimized conformation of NiOEP matched the planar crystal structures of NiOEP as closely as possible. Force constants for substituent groups attached at the periphery of the porphyrin macrocycle were obtained from the general DREIDING II force field so that calculations could be carried out for virtually any substituted porphyrin using the hybrid force field. Van der Waals parameters for the atoms of the macrocycle were taken from the DREIDING II force field and for the substituents were taken from the DREIDING I force field. Partial atomic charges used in calculating the electrostatic contribution to the energy came from application of the charge equilibration method at every 50 iterations during the energy optimization procedure.[25]

This earlier force field has been improved upon slightly for the calculations of the tetrasubstituted porphyrins described herein. The following changes were made in the force field either for consistency with the DREIDING II field, or, more importantly, for improving the ability of the calculations to correctly predict the relative energies of various conformers (local minima) of porphyrins.[26] Firstly, the force field for resonance atom types was modified so that torsions exocyclic to aromatic ring systems (including the porphyrin macrocycle) were reduced to 40% of the value internal to the ring for consistency with DREIDING II.[24] Secondly, an exponential-6 instead of a 12-6 functional form was used for hydrogen atoms; the Lennard-Jones 12-6 functional form was used for all atoms in the previous version of the force field. Finally, DREIDING II parameters were used consistently in the new version of the force field. These changes to the force field parameters required that the equilibrium bond length parameters (and some equilibrium angles parameters) be reoptimized so that the energy-optimized structure of NiOEP matched the crystal structure. The optimization was carried out using the procedure described and developed by Dasgupta.[27] As before, the unconstrained Ni–N bond length (1.855 Å) was not allowed to vary. The reoptimized equilibrium bond lengths are similar to those found by trial and error for the earlier version of the force field.[11] The equilibrium bond lengths and other parameters for the atoms for the new version of the force field are given in Table S1 of the supporting information.

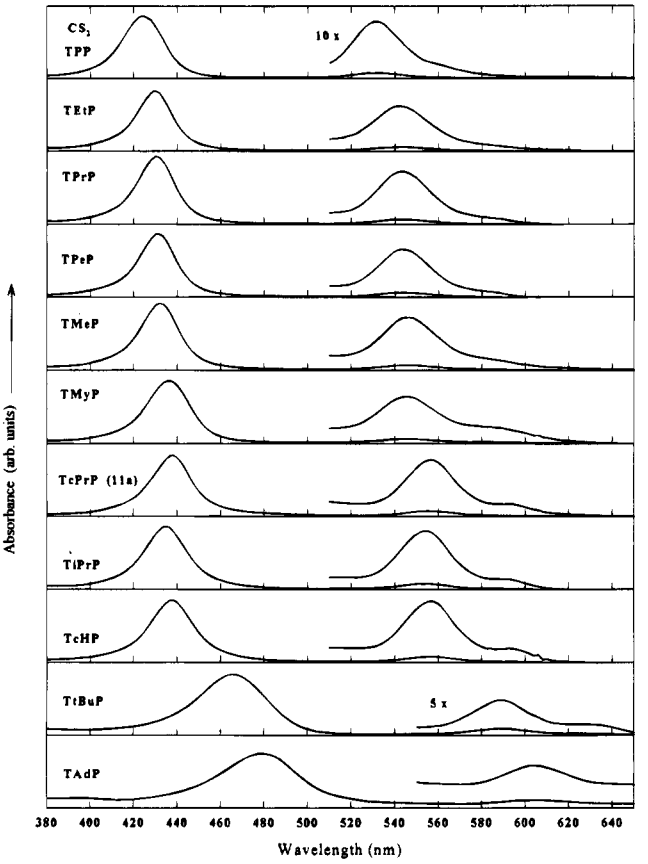

Figure 3. UV–visible absorption spectra of the nickel *meso*-tetrasubstituted porphyrins in carbon disulfide normalized to the Soret band.

Quantum mechanical calculations made use of the INDO/s semiempirical method developed and optimized for spectroscopic predictions by Zerner and co-workers.[28] HyperChem (Hypercube, Inc.) and Argus programs were used for the calculations. The parameter β(d) was varied to give reasonable energies for the d–d transitions for nickel porphyrins, and a value of 32 was chosen. Molecular structures used in the MO calculations were obtained from the classical energy-optimization calculations. The MO calculations were performed on the entire molecular structure, including the substituents, and also, for comparison, on the macrocycle structures calculated for the entire molecule, but with methyl groups replacing the larger *meso*-substituents.

Results

Spectroscopy. The π–π^* transitions of the macrocycle give rise to the bands in the UV–visible region of the absorption spectrum, including the B (Soret) band near 400 nm and the Q_0 and Q_v bands in the red region of the visible spectrum. The UV–visible absorption spectra of the entire series of nickel porphyrins are shown in Figure 3, and the peak wavelengths of the bands are listed in Table 1. Both the B and Q bands progressively red shift as the substituent group becomes more bulky. Thus, *meso*-tetrasubstituted porphyrins with simple linear alkane substituents have the B band near 430 nm and Q_0 and Q_v bands near 540 and 580 nm, respectively. Bulkier substituents like *tert*-butyl and adamantyl give greatly red-shifted spectra with the B band near 470 nm and the Q bands at about

(21) Schrötter, H. W.; Klöckner, H. W. In *Raman Spectroscopy of Gases and Liquids*; Weber, A., Ed.; Springer-Verlag: Berlin, 1979; Chapter 4, p 123.

(22) (a) Torkington, P. *Appl. Spectrosc.* **1980**, *34*, 189. (b) Arora, A. K.; Umadevi, V. *Appl. Spectrosc.* **1982**, *36*, 424.

(23) (a) Li, X.-Y.; Czernuszewics, R. S.; Kincaid, P.; Spiro, T. G. *J. Am. Chem. Soc.* **1989**, *111*, 7012. (b) Li, X.-Y.; Czernuszewics, R. S.; Kincaid, J. R.; Su, Y. O.; Spiro, T. G. *J. Phys. Chem.* **1990**, *94*, 31. (c) Li, X.-Y.; Czernuszewics, R. S.; Kincaid, J. R.; Stein, P.; Spiro, T. G. *J. Phys. Chem.* **1990**, *94*, 47.

(24) Mayo, S. L.; Olafson, B. D.; Goddard, W. A., III. *J. Phys. Chem.* **1990**, *94*, 88.

(25) Rappé, A. K.; Goddard, W. A., III. *J. Phys. Chem.* **1991**, *95*, 3358.

(26) (a) Medforth, C. J.; Senge, M. O.; Forsyth, T. P.; Hobbs, J. D.; Shelnutt, J. A.; Smith, K. M. *Inorg. Chem.* **1994**, *33*, 3865. (b) Medforth, C. J.; Hobbs, J. D.; Rodriquez, M. R.; Abraham, R. J.; Smith, K. M.; Shelnutt, J. A. *Inorg. Chem.* **1995**, in press.

(27) (a) Dasgupta, S.; Goddard, W. A., III. *J. Chem. Phys.* **1989**, *90*, 7207. (b) Yamasaki, T.; Dasgupta, S.; Goddard, W. A., III. *J. Phys. Chem.* **1995**, submitted for publication.

(28) (a) Ridley, J. E.; Zerner, M. C. *Theor. Chim. Acta* **1973**, *32*, 111. (b) Bacon, A.; Zerner, M. C. *Theor. Chim. Acta* **1979**, *53*, 21. (c) Zerner, M. C.; Loew, G. H.; Kirchner, R. F.; Mueller-Westerhoff, U. T. *J. Am. Chem. Soc.* **1980**, *102*, 589. (d) Edwards, W. D.; Weiner, B.; Zerner, M. C. *J. Phys. Chem.* **1988**, *92*, 6188.

Table 1. Wavelength (nm) of the Absorption Band Maxima of the Nickel *meso*-Tetrasubstituted Porphyrins in Carbon Disulfide

Ni porphyrin	Q_0	Q_v	B_0
TPP	561	531.4	423.9
TEtP	578	542.5	429.2
TPrP	579	543.7	429.6
TPeP	577	544.1	430.4
TMeP	584	546.2	431.4
TMyP	586	545.5	435.5
TcPrP ($\alpha\beta\alpha\beta$-**11a**)	592	556.2	437.2
TiPrP	592	553.5	434.6
TcHP	593	555.8	437.3
TtBuP	631	588.7	464.5
TAdP	648	605.3	478.0

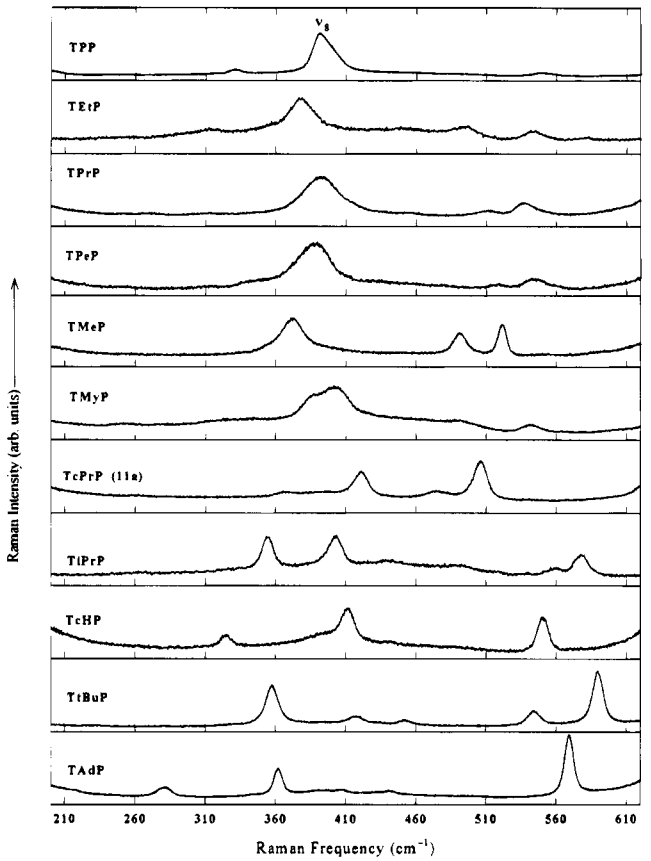

Figure 4. Resonance Raman spectra of the nickel *meso*-tetrasubstituted porphyrins in carbon disulfide in the region from 200 to 600 cm^{-1}. Laser excitation is at 413.1 nm except for NiTtBuP and NiTAdP (457.9 nm).

600 and 650 nm. A marked broadening of the bands is also noted for the bulkiest substituents (Figure 3). This broadening is probably not a result of structural heterogeneity. Also, the intensities of the Q bands increase relative to the B band as the substituents become more bulky; the Q_0 band also gains intensity relative to the Q_v band.

Soret-excited resonance Raman spectra in the low-, middle-, and high-frequency regions for the series of nickel porphyrins in solution are shown in Figures 4−6, and the frequencies for some of the structure-sensitive lines are listed in Table 2. The low-frequency region (200−600 cm^{-1}) serves as a fingerprint region for identifying the particular substituent. Even subtle differences in the substituents give rise to significant differences in the spectra as shown by a comparison of the spectra of the methyl, ethyl, propyl, and pentyl derivatives in this region. The low-frequency region also contains the ν_8 vibrational mode which consists primarily of the Ni−N and $C_\alpha-C_m$ bond stretching motion and methine bridge bending[23b] and which is also structure sensitive in a complicated way. The mid-

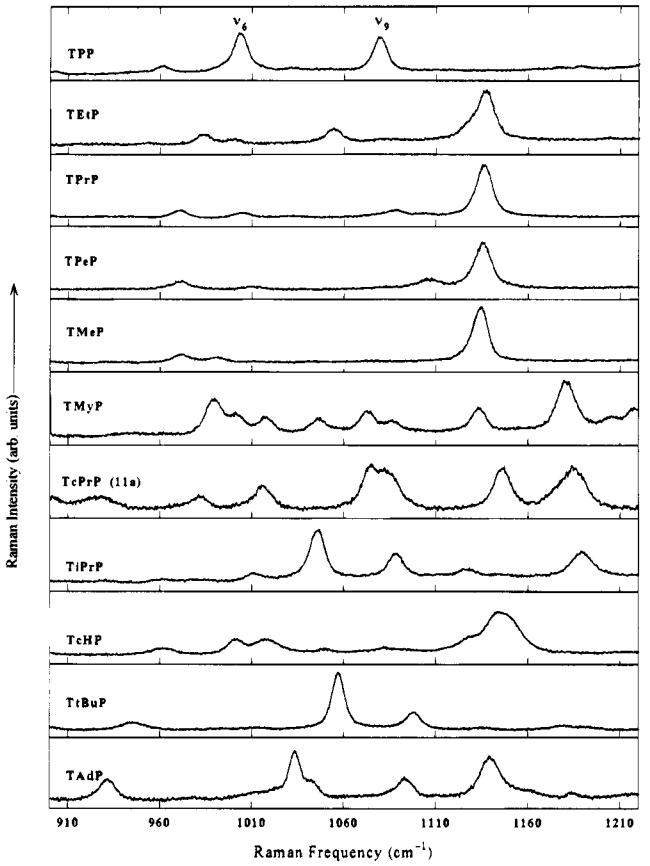

Figure 5. Resonance Raman spectra of the nickel *meso*-tetrasubstituted porphyrins in carbon disulfide in the region from 900 to 1200 cm^{-1}. Laser excitation is at 413.1 nm except for NiTtBuP and NiTAdP (457.9 nm).

frequency region from 900 to 1200 cm^{-1} also is highly variable depending on the type of substituent and contains the ν_6 (N−C_α stretching, pyrrole breathing) and ν_9 (C_β−H bending) vibrational modes of the macrocycle.[23b]

The high-frequency region between 1300 and 1600 cm^{-1} (Figure 6) contains the well-known structure-sensitive Raman lines.[11,29] These lines include the oxidation-state marker line ν_4 and the so-called core-size marker lines ν_3, ν_{28}, and ν_2. These lines decrease in frequency with the size of the *meso*-substituent. (Also see Figure 7a,b.) Some structural heterogeneity is in evidence in the broadness and asymmetry of the structure sensitive lines, for ν_2 in particular.

Resonance Raman spectra of powder samples for some of the porphyrins are shown in Figure S1 in the supporting information, and the structure-sensitive marker line frequencies are given in Table 2. Significant differences in the frequencies of the structure-sensitive lines between powder and solution spectra are noted only for NiTMyP and NiTcHP.

Molecular Modeling. Molecular mechanics calculations show that *meso*-tetrasubstituted porphyrins generally take on a ruffled conformation (B_{1u} distortion). The calculated lowest energy conformations for some of the tetrasubstituted porphyrins are shown in Figure 8. The ruffling dihedral angle and several other important structural parameters, including the core size,

(29) (a) Yamamoto, T.; Palmer, G.; Gill, D.; Salmeen, I. T.; Rimai, L. *J. Biol. Chem.* **1973**, *248*, 5211. (b) Spiro, T. G.; Strekas, T. C. *J. Am. Chem. Soc.* **1974**, *96*, 338. (c) Kitagawa, T.; Ogoshi, H.; Watanabe, E.; Yoshida, Z. *J. Phys. Chem.* **1975**, *79*, 2629. (d) Spaulding, L. D.; Chang, C. C.; Yu, N.-T.; Felton, R. H. *J. Am. Chem. Soc.* **1975**, *97*, 2517. (e) Stong, J. D.; Spiro, T. G.; Kubaska, R. J.; Shupack, S. I. *J. Raman Spectrosc.* **1980**, *9*, 312. (f) Parthasarathi, N.; Hansen, C.; Yamaguchi, S.; Spiro, T. G. *J. Am. Chem. Soc.* **1987**, *109*, 3865. (g) Czernuszewicz, R. S.; Li, X.-Y.; Spiro, T. G. *J. Am. Chem. Soc.* **1989**, *111*, 7024. (h) Prendergast, K.; Spiro, T. G. *J. Am. Chem. Soc.* **1992**, *114*, 3793.

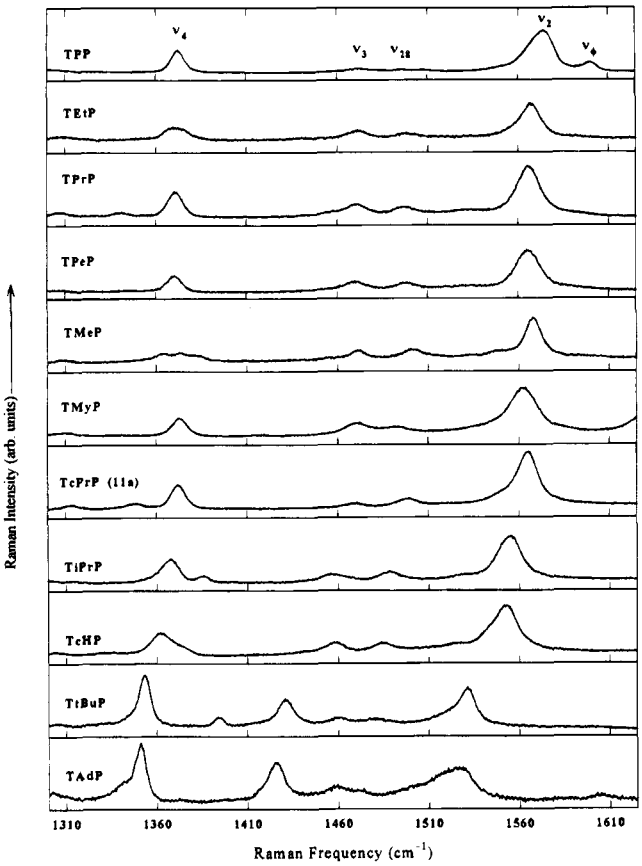

Figure 6. Resonance Raman spectra of the nickel *meso*-tetrasubstituted porphyrins in carbon disulfide in the region from 1300 to 1600 cm^{-1}. Laser excitation is at 413.1 nm except for NiTtBuP and NiTAdP (457.9 nm).

Table 2. Frequencies (cm^{-1}) of Selected Resonance Raman Lines for the Nickel *meso*-Tetrasubstituted Porphyrins in Solution and Powder (in Parentheses)

Ni porphyrin	ν_2, p[a]	ν_3, p	ν_4, p	ν_8, p	ν_{28} or ν_{11}, dp[a]
TPP	1574.8	1472.9	1373.3	391.9	1486
TEtP	1567.5	1470.3	1367.5	377.7	1498.9
TPrP	1565.2	1470.3	1370.4	391.9	1496.0
TPeP	1565.6	1470.1	1370.8	386.9	1497.6
	(1569)	(1471)	(1371)	(394)	(1497)
TMeP	1567.7	1470.7	1362.9	371.3	1501.4
TMyP	1562.0	1471.0	1372.9	386/403	1493.0
($\alpha\beta\alpha\beta$, $\alpha^2\beta^2$)	(1556)	(1467)	(1373)	(388/408)	(1487)
TCPrP $\alpha\beta a\beta$-**11a**	1565.0	1470.0	1372.0	420.8	1499.0
TiPrP	1553.9	1456.1	1366.6	400.5	1487.9
	(1554)	(1457)	(1365)	(399)	(1486)
TcHP	1551.9	1457.8	1361.9	411.3	1484.7
	(1557)	(1462)	(1362)	(406)	(1486)
TtBuP	1532.8	1432.3	1354.5	358.4	1461.9
	(1532)	(1432)	(1353)	(363)	(1462)
TAdP	1526.0	1425.2	1350.8	361.7	1458.6

[a] p indicates a polarized Raman line; dp indicates a depolarized Raman line.

are given for the porphyrins of the series in Table 3. Generally, the degree of nonplanar distortion depends on the size of the *meso* substituent, as can be seen in the increase in the ruffling dihedral angle. The calculated ruffling dihedral angle ($C_\alpha N-NC_\alpha$ for nitrogens in opposite pyrroles) reaches 57° for the most distorted porphyrin (NiTAdP).

Most of the porphyrins form stable conformers at higher energy (local minima); these conformers exhibit a symmetric distortion that is different from the most stable B_{1u}-symmetry (*ruf*) distortion. Figures 9, 10, and S2 (supporting information) show these high-energy conformers, as well as the lowest energy *ruf* conformer, for NiTEtP and NiTtBuP. The energies of these conformers, along with the energies of selected conformers of NiTMeP and NiTMyP, are listed in Table 4.

Figure 11 compares the calculated structure and the X-ray crystallographic structure of nickel(II) *meso*-tetraisopropylporphyrin.[14] The root-mean-square deviation between the calculated and experimental structures is 0.112 Å for the 25 atoms of the macrocycle and 0.121 Å for the 37 metal, carbon, and nitrogen atoms of NiTiPrP. The ruffling dihedral angle is 36.6° for the calculated structure and 43.7° for the X-ray structure. The average $NC_\alpha C_m C_\alpha$ torsion angles are 17.7° (calculated) and 12.6° (X-ray), and the $NC_\alpha C_\beta C_\beta$ torsion angles are 1.5° (calculated) and 3.0° (X-ray). Therefore, the calculations underestimate the ruffling dihedral angle and the $C_\alpha C_\beta$ torsion angle and overestimate the $C_\alpha C_m$ torsion angle. These discrepancies might be a result of crystal packing forces not considered in the calculations; however, we do not believe this to be the case (*vide infra*).

For other nickel tetrasubstituted porphyrins, the agreement between the crystal structures and the calculated structures is not as good. For example, NiTMyP crystallizes with two distinct molecules in the unit cell with $C_\alpha N-NC_\alpha$ angles of 42.6° and 48.6° for the $\alpha\beta\alpha\beta$ and $\alpha^2\beta^2$ conformers, respectively.[18] The $NC_\alpha C_m C_\alpha$ torsion angles are 11.2° and 12.6° and the $NC_\alpha C_\beta C_\beta$ torsion angles are 3.7° and 3.6°, respectively, for the $\alpha\beta\alpha\beta$ and $\alpha^2\beta^2$ conformers in the crystal. The molecular mechanics calculations give only 26.4° for the ruffling angle and 12.7° and 1.2° for the torsion angles for the $\alpha\beta\alpha\beta$ atropisomer, and for the $\alpha^2\beta^2$ conformer, 10.8° for the ruffling angle and 5.5° and 1.6° for the torsion angles. For NiTMyP, the large discrepancies between the crystal structures and the calculated structures are probably in part due to crystal packing forces. The differences in the resonance Raman data for NiTMyP in solution and in powder support this view. The frequency of ν_2 is 6 cm^{-1} lower in the crystal Raman spectrum than in the solution spectra (Table 2). Similarly, other lines sensitive to ruffling downshift, indicating a significantly more ruffled structure for NiTMyP in the crystalline state. Because of the absence of packing forces, the solution conformation should more closely match the calculated structure of the molecule in vacuum, and this is the case.

Nevertheless, there remains additional evidence for a systematic errors in the predictions of the energy-minimized structures. In the X-ray structure of NiTcHP,[17] the angles are 46.2°, 13.8°, and 3.0° and the corresponding calculated angles are 37.8°, 18.3°, and 1.6°. Thus, these calculations also consistently underestimate the ruffling angle and the torsion in the $C_\alpha C_\beta$ bond and overestimate the torsion in the $C_\alpha C_m$ bond for all of these porphyrins (NiTiPrP, NiTMyP, and NiTcHP). Therefore, a systematic inaccuracy in the calculated structures is likely.

For NiTMeP, five crystal structures have been reported, two neutral forms, two radical cations, and a crystal partially oxidized with iodine.[30] As might be expected on the basis of the small difference (3.5 kcal mol^{-1}) between the *ruf* and planar (constrained) conformers (see Table 4), both planar and nonplanar conformers are observed. A planar conformer is observed for the NiTMeP radical cation in $[NiTMeP]_2[ReO_4]$;[30f] two other crystals (partially oxidized NiTMeP and $[NiTMeP]_2[PF_6]$) have fairly nonplanar conformations that are approximately equal

(30) (a) Gallucci, J. C.; Swepston, P. N.; Ibers, J. A. *Acta Crystallogr.* **1982**, *38*, 2134. (b) Pace, L. J.; Ulman, A.; Ibers, J. A. *Inorg. Chem.* **1982**, *21*, 199. (c) Kutzler, F. W.; Swepston, P. N.; Berkovitch-Yellin, Z.; Ellis, D. E.; Ibers, J. A. *J. Am. Chem. Soc.* **1983**, *105*, 2996. (d) Pace, L. J.; Martinsen, A.; Ulman, A.; Hoffman, B. M.; Ibers, J. A. *J. Am. Chem. Soc.* **1983**, *105*, 2612. (e) Newcomb, T. P.; Godfrey, M. R.; Hoffman, B. M.; Ibers, J. A. *J. Am. Chem. Soc.* **1989**, *111*, 7078. (f) Newcomb, T. P.; Godfrey, M. R.; Hoffman, B. M.; Ibers, J. A. *Inorg. Chem.* **1990**, *29*, 223.

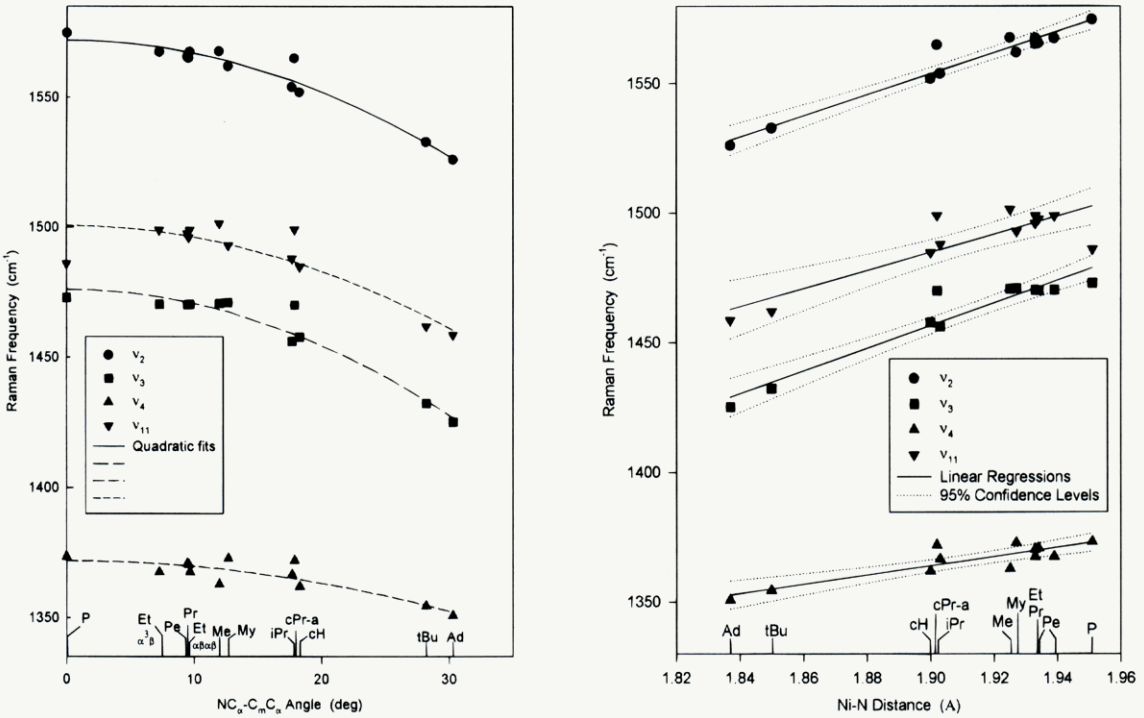

Figure 7. Frequencies of some structure-sensitive Raman lines as a function of the calculated average $NC_\alpha-C_mC_\alpha$ dihedral angle (left) and Ni−N distance (right).

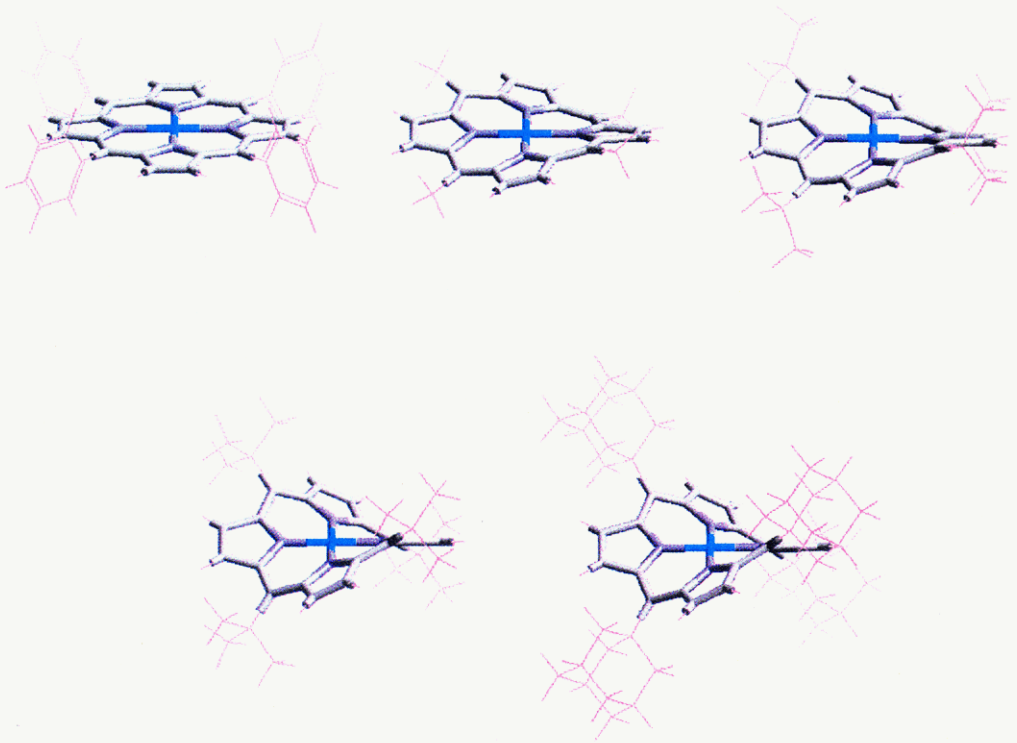

Figure 8. Calculated lowest energy conformations of some of the series of nickel(II) tetrasubstituted porphyrins: tetraphenylporphyrin (top left), tetramethylporphyrin (top center), tetraisopropylporphyrin (top right), tetra-*tert*-butylporphyrin (bottom left), and tetraadamantylporphyrin (bottom right). The degree of ruffling increases with the steric bulk of the substituents.

mixtures of the *ruf* and *sad* distortions;[30d,e] the structure of neutral NiTMeP with the $\pi-\pi$ complexing agent TCNQ is slightly nonplanar with a mixture of the *ruf* and *wav* distortions,[30b] and yet another crystal of neutral NiTMeP exhibits a slight *wav* distortion.[30a,c] No completely planar neutral NiTMeP crystal structures are known. Clearly, the packing forces and methyl orientations play dominant roles in determining the conformation of NiTMeP in the crystalline state.

INDO/s calculations were performed using the lowest energy conformations of the nickel tetrasubstituted porphyrins obtained from molecular mechanics calculations. The predicted energies of the singlet $\pi \rightarrow \pi^*$ transitions associated with the B and Q bands are given in Figure 12 as a function of the calculated ruffling dihedral angle. The red shifts in the transition energies with the degree of ruffling are accurately predicted even though the absolute calculated energies are significantly different from the experimentally measured transition energies. The energies of the lowest unoccupied molecular orbitals (LUMOs) and highest occupied molecular orbitals (HOMOs) are plotted in Figure S3 of the supporting information.

Table 3. Selected Structural Parameters Obtained from Calculated Conformations and Crystal Structures (in Parentheses)

Ni porphyrin	core size (Å)	dihedral angle (deg)	$C_\alpha NC_\alpha$ angle (deg)	N−Ni−N angle (deg)	$C_\beta-C_\beta$ bond (Å)	$C_\alpha-C_m$ bond (Å)	$C_\alpha-N$ bond (Å)	$XC_\alpha-C_mX$ angle (deg)	$NC_\alpha-C_\beta C_\beta$ angle (deg)
TPP	1.951	0.1	104.4	180.0	1.320	1.383	1.386	0.0	0.0
TEtP									
ruf $\alpha\beta\alpha\beta$	1.933	21.0	104.9	180.0	1.321	1.388	1.386	9.7	1.3
ruf $\alpha^3\beta$	1.939	16.2	104.8	179.2	1.319	1.388	1.388	7.3	1.2
dom α^4	1.949	0.9	104.6		1.317	1.388	1.389	3.6	0.9
wav $\alpha^2\beta^2$	1.948	0.4	104.6		1.317	1.388	1.389	3.4	1.0
TPrP	1.933	20.9	104.9	180.0	1.320	1.388	1.386	9.6	1.3
TPeP	1.934	20.8	104.9	180.0	1.320	1.388	1.386	9.5	1.3
TMeP									
ruf	1.925	25.3	105.1	180.0	1.323	1.388	1.384	12.0	1.1
(*ruf* + *sad*)[a]	(1.938)	(17.0)	(105.2)	(174.0)	(1.339)	(1.388)	(1.382)	(6.9)	(1.6)
TMyP									
ruf $\alpha\beta\alpha\beta$	1.927	26.4	105.2	179.9	1.321	1.387	1.385	12.7	1.2
(*ruf*)[b]	(1.898)	(42.6)	(106.5)	(179.1)	(1.338)	(1.381)	(1.376)	(11.2)	(3.7)
ruf $\alpha^2\beta^2$	1.946	10.8	104.7	179.9	1.316	1.390	1.390	5.5	1.6
(*ruf*)[b]	(1.894)	(48.6)	(106.8)	(178.8)	(1.341)	(1.390)	(1.370)	(12.6)	(3.6)
wav $\alpha^2\beta^2$	1.950	0.4	104.6	179.9	1.315	1.387	1.390	5.7	1.7
TcPrP $\alpha\beta\alpha\beta$-**11a**	1.902	35.3	105.6	180.0	1.327	1.387	1.380	17.9	0.7
TiPrP									
ruf	1.903	36.6	105.9	179.9	1.324	1.393	1.384	17.7	1.5
(*ruf*)[c]	(1.896)	(43.7)	(106.1)	(177.9)	(1.343)	(1.392)	(1.393)	(12.6)	(3.0)
TcHP									
ruf	1.900	37.8	105.9	179.9	1.324	1.393	1.384	18.3	1.6
(*ruf*)[d]		(46.2)						(13.8)	(3.0)
TtBuP	1.850	53.2	107.5	180.0	1.330	1.401	1.379	28.2	0.1
TAdP	1.837	56.6	107.9	180.0	1.332	1.403	1.377	30.3	0.7

[a] Partially oxidized NiTMeP iodide crystal structure from ref 30d. [b] NiTMyP crystal structure, ref 18. [c] NiTiPrP crystal structure, ref 14. [d] NiTcHP crystal structure ref 17.

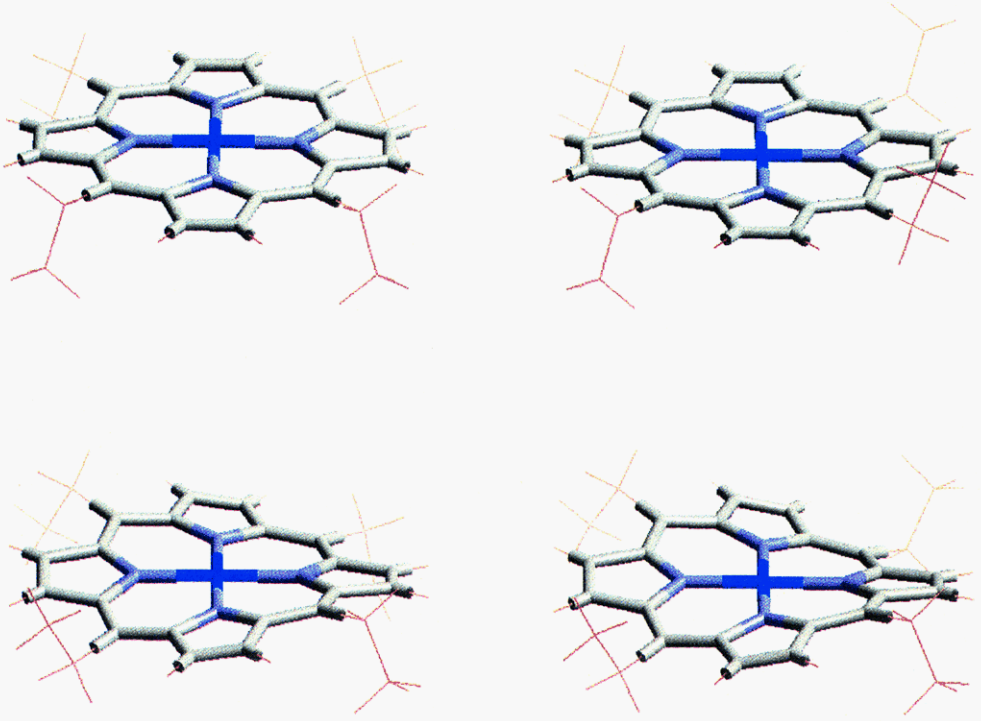

Figure 9. Calculated conformations of nickel tetraethylporphyrin with the four possible ethyl orientations: α^4 (top left), $\alpha^3\beta$ (bottom left), $\alpha^2\beta^2$ (top right), and $\alpha\beta\alpha\beta$ (bottom right). The α^4 conformer shows a slight *dom* (A_{2u}) distortion; the $\alpha^2\beta^2$ conformer a small *wav* (E_g) distortion; the other two conformers exhibit varying degrees of the *ruf* (B_{2u}) distortion.

Discussion

Symmetric Nonplanar Distortions of Porphyrins. Nonplanar distortions of the porphyrin macrocycle are commonly observed in crystallographic structures[31−33] and have been detected spectroscopically in environments other than in the crystalline phase.[3,9,29g,33] A planar porphyrin is typically favored because of the aromatic conjugated bonds of the macrocycle. However, nonplanar distortions are likely for small metals like (low-spin) nickel(II) because a nonplanar distortion generally shortens the metal−nitrogen(pyrrole) bond distance. Also, peripheral substitution of the porphyrin can lead to nonplanar distortions that act to relieve the steric crowding of the substituents. For symmetrically substituted porphyrins, often

(31) Meyer, E. F. *Acta Crystallogr., Sect. B* **1972**, *28*, 2162.
(32) Barkigia, K. M.; Berber, M. D.; Fajer, J.; Medforth, C. J.; Renner, M. W.; Smith, K. M. *J. Am. Chem. Soc.* **1990**, *112*, 8851.
(33) (a) Gellin, B. R.; Karplus, M. *Proc. Natl. Acad. Sci. U.S.A.* **1977**, *74*, 801. (b) Berghuis, A. M.; Brayer, G. D. *J. Mol. Biol.* **1992**, *214*, 959.

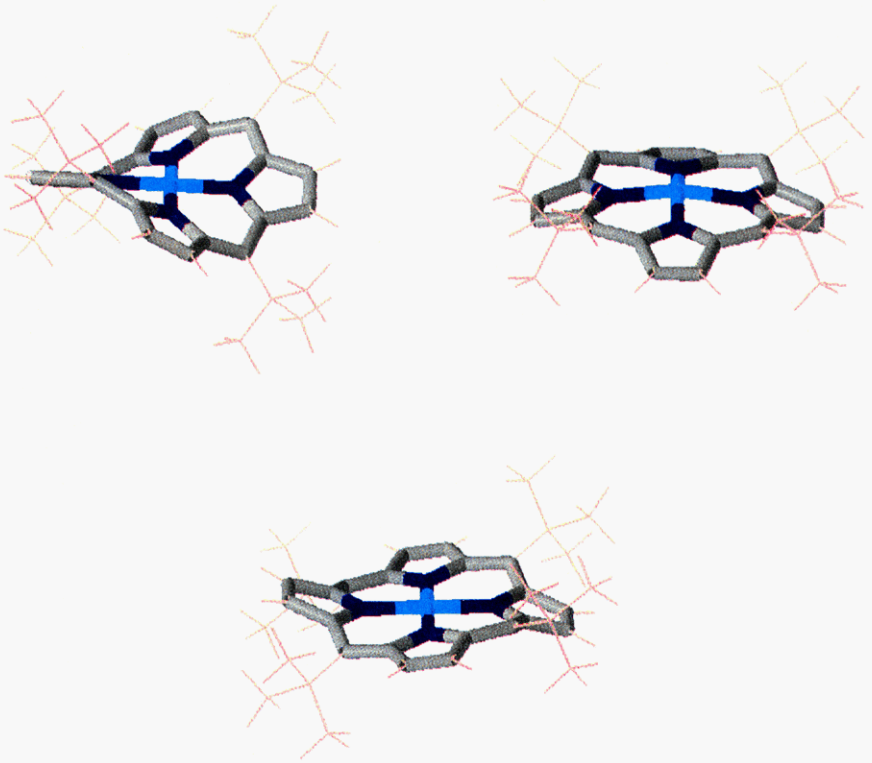

Figure 10. Calculated conformations of nickel tetra-*tert*-butylporphyrin obtained by initiating minimization from a planar macrocycle with the *tert*-butyl substituents in the α^4, $\alpha^3\beta$, $\alpha^2\beta^2$, and $\alpha\beta\alpha\beta$ orientations. For both the $\alpha^3\beta$ and $\alpha\beta\alpha\beta$ orientations, the *ruf* conformer results (top left); for the α^4 conformer, a *dom* conformation is found (top right); and for the $\alpha^2\beta^2$ conformer, a *wav* conformation (bottom) is found.

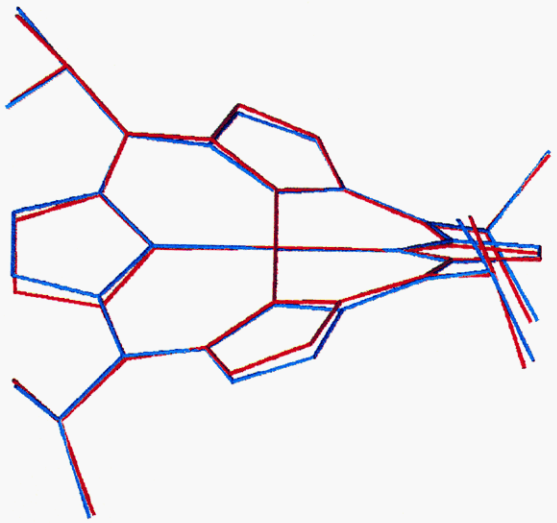

Figure 11. Comparison of the calculated (blue) and X-ray crystal (red) structures of nickel tetraisopropylporphyrin. The root-mean-square difference between the positions of the atoms in the two structures is 0.121 Å. Most of the error results from an asymmetrical nonplanar distortion, in addition to the ruffling, observed for the crystal structure.

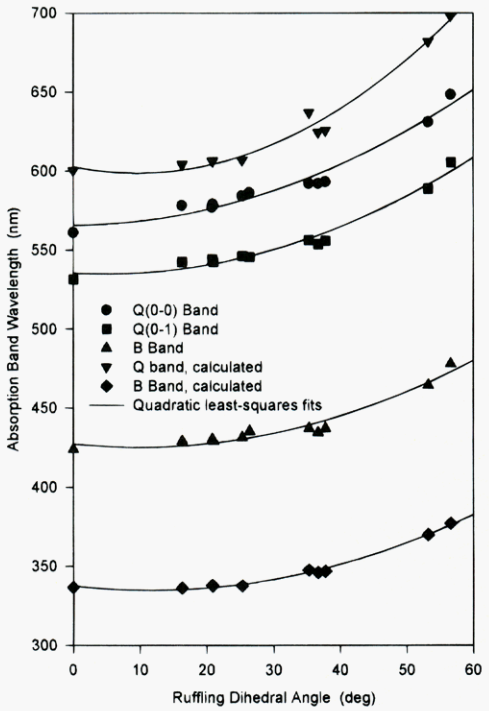

Figure 12. Wavelength of the experimental and INDO/s calculated transition energies of the nickel tetrasubstituted porphyrins as a function of the ruffling angle: B band, calculated (◆), measured (▲); Q_v band, measured (■); Q_0 band, calculated (▼), measured (●).

the nonplanar distortion that occurs is itself symmetrical and can be classified according to the irreducible representations of the nominal D_{4h} point group of a square-planar porphyrin. Two most commonly observed distortions are the *ruf* distortion which belongs to the B_{1u}-symmetry classification and the *sad* distortion which belongs to the B_{2u}-symmetry classification. The *ruf* distortion involves a twisting about the metal−nitrogen bond, and the best known example is the ruffled crystal structure of NiOEP.[31] The *sad* distortion involves the displacement of the pyrrole rings alternately above and below the mean porphyrin plane so that the pyrrole nitrogens are out of the mean plane. A good example of the saddling distortion is seen in the crystal structure of metal octaethyltetraphenylporphyrins (MOETPPs).[4,32]

These B_{1u} and B_{2u} nonplanar distortions roughly correspond to nonplanar vibrational deformations of the square-planar (D_{4h} symmetry) macrocycle that occur in the two lowest frequency normal modes of the macrocycle with these symmetries. For example, the lowest frequency normal mode of B_{1u} symmetry

(γ_{14}) is calculated to be at 44 cm^{-1} for NiOEP;[23a] the relative magnitudes and directions of the out-of-plane displacements of the atoms for this mode are almost identical to the displacements observed in the crystals of porphyrins exhibiting the static *ruf* distortion. Similarly, the displacements of the atoms in the lowest B_{2u} normal mode (γ_{18}), calculated to be at 30 cm^{-1},[23a] resemble the displacements observed for the static *sad* distortion. It is not surprising that symmetric distortions akin to these normal modes are the most commonly observed, inasmuch as these are two of the softest modes of deformation of the porphyrin macrocycle, *i.e.*, the restoring forces for distortions along these normal coordinates are smallest. The energy of a vibrational quantum for these normal modes (<50 cm^{-1}) is much less than k_BT at room temperature (206 cm^{-1}), and thus perturbations of only small energies ($\sim k_BT$) can easily cause distortions along these normal coordinates of many times the root-mean-square amplitude of vibration.

Another frequently observed symmetrical nonplanar distortions is the doming (*dom*) distortion corresponding to the lowest A_{2u} normal mode (γ_9) calculated to be at 32 cm^{-1} (see Figure 2b). This distortion is often observed in five-coordinate complexes when the axial ligand causes a displacement of the metal out of the mean plane. It also occurs in six-coordinate complexes with different axial ligands. A good example is the doming of the heme that occurs in deoxyhemoglobin.[34]

An occasionally observed nonplanar distortion of porphyrins corresponds to the waving (*wav*) deformation that takes place in the lowest E_g mode (γ_{26}). This doubly-degenerate normal mode is calculated to appear at significantly higher frequency (63 cm^{-1}) than the lowest B_{1u}, B_{2u}, and A_{2u} modes, and thus the restoring force for distortion along this normal coordinate is stronger. Consequently, static distortion along this normal coordinate requires a greater external perturbation upon the nominally planar porphinato macrocycle to produce the same degree of distortion as for one of the other symmetric distortions. Nevertheless, distortions corresponding to the E_g mode are observed in some crystal structures, including two of the NiTMeP structures.[35,30a,b] This distortion is also encountered in molecular mechanics calculations either as the lowest energy structure or, more often, as a less stable conformer (local minimum) of porphyrins whose lowest energy conformer is one of the more common B_{1u}, B_{2u}, or A_{2u} type. Symmetric distortions corresponding to other out-of-plane normal modes are possible but would require perturbations of even higher energy.

The foregoing discussion provides a convenient and consistent framework for classifying and distinguishing symmetric nonplanar distortions of porphyrins. Obviously, nonplanar distortions of the macrocycle occur that do not directly correspond to any of these symmetric deformations. In many cases, however, the distortion can be described as a combination of two or more of the four symmetrical distortions described above. One commonly observed distortion of this type is a mixture of the *ruf* and *sad* distortions; the crystal structures observed for two of the NiTMeP crystals[30d,e] and some metallotetraphenylporphyrins[36] are examples. Furthermore, viewing a nonplanar distortion in terms of deformations along the soft normal coordinates of the molecule provides a useful means of rationalizing or even predicting the structural consequences of a particular perturbation. That is, the deformation that most efficiently relieves the steric repulsion will be observed (*vide infra*).

Nonplanar Distortions of the Tetrasubstituted Porphyrins. Tetrasubstituted porphyrins, with either a single atom or else a nonplanar substituent group attached at the *meso* carbons, generally exhibit the *ruf* distortion. (This applies to all of the porphyrins in this study except NiTPP.) The reason that the *ruf* distortion is favored is that only a small movement of the *meso* substituent out of plane is sufficient to relieve the quasi-equatorial steric interaction between the substituent atom directly bonded to the *meso* carbon and the adjacent pyrrole rings. As a consequence of the out-of-plane displacement of the substituent atoms, the *meso* carbons of the porphyrin follow, giving the out-of-plane displacement of the *meso* carbons that is characteristic of the B_{1u} distortion (Figure 2a). Free rotation of tetrahedrally-bonded atoms (*e.g.*, alkyl substituents) at the *meso* carbons also helps to removes strain efficiently without much displacement out of plane. Thus, the *ruf* distortion is more favored relative to the *sad* distortion for sp^3-bonded substituents at the *meso* positions.

The *sad* distortion is most commonly observed when the porphyrin is fully substituted with 12 bulky groups, especially when the four *meso* substituents are planar sp^2-bonded groups.[32] For planar substituents like phenyl or nitro groups at the *meso* carbons, a much larger out-of-plane displacements is required to relieve the steric strain because the entire group must move out of plane. This is not the case for an sp^3 atom at the *meso* carbon. Apparently, the out-of-plane displacement of the entire pyrrole ring that occurs in the *sad* distortion removes the peripheral steric strain more efficiently than the large displacements of the *meso* substituents that would be required to relieve the strain by way of the *ruf* distortion. (For the B_{2u} distortion, the *meso* carbons remain in the mean porphyrin plane, in contrast with the B_{1u} distortion.)

These general rules for predicting the type of nonplanar distortion are based on the relative efficacy of distortions along the soft normal coordinates in relieving steric interactions between substituents. These rules are generally confirmed by examination of the extensive X-ray crystallographic data of symmetrically substituted porphyrins. Using these rules, we chose a series of *meso*-tetrasubstituted nickel porphyrins with mostly alkyl substituents as models for the predominantly *ruf*-distorted heme of cytochrome *c*. The alkyl substituents were chosen because they have similar inductive properties; thus, changes in the spectral and chemical properties are primarily a result of nonplanar distortions and steric differences along the series and not direct electronic differences resulting from differing electron withdrawing/donating properties of the substituents.

Molecular Mechanics Calculations. As expected, the molecular mechanics calculations show that the lowest energy conformation for every porphyrin of the series is the *ruf* conformation (except NiTPP, which is nearly planar). Further, the degree of distortion, as measured by the ruffling dihedral angle, roughly follows the size of the substituent group. One notable exception is the methyl derivative which is more ruffled (25°) than the porphyrins with the larger linear alkanes (16–21°). This anomaly probably results from the added rotational freedom of the methyl group that is not shared by the longer linear alkyl substituents. In fact, depending on the starting orientations of the linear alkyl groups, several low-energy conformers with varying ruffling angles are predicted by the molecular mechanics calculations for these porphyrins. For NiTEtP for example, the ruffling dihedral angle varies from 1° for the α^4 conformer to 21° for the lowest energy $\alpha\beta\alpha\beta$

(34) (a) Deatherage, J. F.; Loe, R. S.; Anderson, C. M.; Moffat, K. *J. Mol. Biol.* **1976**, *104*, 687. (b) Ladner, R. C.; Heidner, E. J.; Perutz, M. F. *J. Mol. Biol.* **1977**, *114*, 385. (c) Takano, T. *J. Mol. Biol.* **1977**, *110*, 537.

(35) Nurco, D.; Forsyth, T.; Medforth, C. J.; Smith, K. M.; Shelnutt, J. A. Unpublished results. The free base of a fluorinated dodecaphenylporphyrin (H_2DPPF_{28}) shows a more pronounced *wav* distortion.

(36) (a) Fleischer, E. B.; Miller, C. K.; Webb, L. E. *J. Am. Chem. Soc.* **1964**, *86*, 2342. (b) Madura, P.; Scheidt, W. R. *Inorg. Chem.* **1976**, *15*, 3182. (c) Stevens, E. D. *J. Am. Chem. Soc.* **1981**, *103*, 5087.

conformer. The calculated structures of the four NiTEtP conformers are shown in Figures 9 and S2 (supporting information). The additional van der Waals interactions between the methyl group of the ethyl substituents and the adjacent pyrrole rings, not present for NiTMeP, account for the different structures and also for NiTEtP's markedly less ruffled structure compared to that of the tetramethylporphyrin derivative.

One shortcoming of the molecular mechanics calculations should be mentioned at this point. In many cases, Ni porphyrins are known to coexist in solution in both planar and nonplanar forms. NiOEP is an example. NiOEP is also known to exist in different crystalline forms as either a planar or ruffled conformer.[31,37] Unfortunately, our energy-optimization calculations for NiOEP give only the planar conformer. That is, the calculations do not predict a barrier between the planar and ruffled NiOEP conformers, although they do predict that the conformers would be close in energy. Thus, for the Ni tetrasubstituted porphyrins with small *meso* substituents, and therefore not much steric crowding at the periphery, either a planar or a nonplanar conformer or both conformers might be observed. Furthermore, the degree of ruffling observed for the methyl and linear alkyl porphyrin derivatives in crystals may be expected to differ from the lowest energy structure predicted by the molecular mechanics calculations. And, because the energies for different conformers do not differ substantially, we may also expect the nonplanarity to depend on solvent or other environmental conditions. Specifically, the predicted weak preference for a ruffled conformer for the porphyrins with *normal* alkyl substituents can be overcome by packing forces in the crystalline phase; consequently, either a planar or a nonplanar conformer might be found. Thus, as for NiOEP,[31,37] the Ni tetraalkylporphyrins may show different degrees of nonplanarity of the macrocycle in the environment of the crystal. This is known to be the case for NiTMeP[30] and NiTPrP,[38] which exhibit planar or nonplanar conformers in various crystalline forms. Similar arguments also imply that there will be heterogeneity in the degree of nonplanarity for solutions of the *meso*-tetrasubstituted porphyrins with the smallest alkyl substituents.

Different substituent orientations can also result in different conformers and mixtures of conformers in solution. For example, the calculations for NiTEtP give the energies of the $\alpha^2\beta^2$, α^4, and $\alpha^3\beta$ conformers (141.4, 141.3, and 140.7 kcal mol^{-1}, respectively) all within 1.7 kcal mol^{-1} of the most stable $\alpha\beta\alpha\beta$ conformer at 139.7 kcal mol^{-1} (see Figure 9). All conformers are within several k_BT at room temperature; therefore, they coexist in solution, with the more ruffled forms weakly favored.

Multiple conformers are also calculated for NiTtBuP, but in this case, the energies of the conformers differ greatly in energy because steric interaction is larger than for NiTEtP (Figure 10 and Table 4). The conformers are calculated by starting the energy-optimization calculation from a conformation with a planar macrocycle and the *tert*-butyl groups oriented in one of either the α^4, $\alpha^3\beta$, $\alpha^2\beta^2$, or $\alpha\beta\alpha\beta$ configurations. The *ruf* conformer is the lowest in energy. After the macrocycle is in one of the conformations shown in Figure 10, rotation of the *tert*-butyl substituents to another configuration is not enough to convert to one of the other conformers. This suggests that large energy barriers exist for interconversion between the stable conformers (estimated to be up to 50 kcal mol^{-1} for the *ruf* to *dom* interconversion). Conversion to high-spin nickel(II) greatly lowers the energetic differences between these conformers (Table 4) because the larger core of these conformers more readily accepts the large high-spin nickel(II) ion.

Table 4. Energies (kcal/mol) of the Low- and High-Spin Nickel Porphyrin Conformers for Tetra-*tert*-butylporphyrin and Tetraethylporphyrin

	low spin (1.855 Å)			high spin (2.070 Å)		
conformer	conformer type	energy	relative energy	conformer type	energy	relative energy
NiTtBuP						
$\alpha\beta\alpha\beta$	*ruf*	127.9	0.0	*ruf* + *dom*	138.8	0.0
$\alpha^2\beta^2$	*wav*	156.4	28.5	*wav*	155.5	16.7
$\alpha^3\beta$	*ruf*	127.9	0.0	*ruf* + *dom*	138.8	0.0
α^4	*dom*	153.2	25.3	*dom*	146.1	7.3
NiTEtP						
$\alpha\beta\alpha\beta$	*ruf*	139.7	0.0	*ruf*	134.8	0.0
$\alpha^2\beta^2$	*wav*	141.4	1.7	*wav*	135.1	0.3
$\alpha^3\beta$	*ruf*	140.7	1.0	*ruf* + *dom*	135.0	0.2
α^4	*dom*	141.3	1.6	*dom*	134.9	0.1
NiTMyP						
$\alpha\beta\alpha\beta$	*ruf*	425.6	0.0			
$\alpha^2\beta^2$	*wav*	429.1	3.5			
	ruf	429.2	3.6			
NiTMeP	*ruf*	119.5	0.0			
	planar	123.0	3.5			

Resonance Raman Spectra and Frequency−Structure Relationships. The resonance Raman spectra contain a wealth of information about the molecular structure and conformation of the tetrasubstituted porphyrins. For example, the Raman lines in the low- and mid-frequency ranges are sensitive to peripheral substitution and thus provide a fingerprinting method for identifying the nature of the peripheral substituents of this series of nickel porphyrins. There is also hope for using these regions of the Raman spectra for distinguishing between different nonplanar conformations when symmetric distortions other than the *ruf* distortion studied herein have been characterized.

The high-frequency region contains the structure-sensitive in-plane vibrations. These modes are known to be sensitive to oxidation state,[29a,b] core size,[29d−f] nonplanar distortion,[29g,h] axial ligands,[29c] and spin state.[29b] For the nickel tetrasubstituted porphyrins, the nickel ion's oxidation state and spin state are the same for the entire series. The marker lines in this case are sensitive to the magnitude of the nonplanar distortion and the resulting change in the core size. However, the core size variation in the frequencies is not that originally observed for planar porphyrins with different metals (anti-correlation)[29d] but one that results from varying degrees of nonplanarity (correlation, Figure 7b).[11,39]

Figure 7a shows the dependence of the frequency of several Raman lines on the degree of nonplanarity as measured by the torsion angle for the $C_\alpha-C_m$ bond. The $C_\alpha-C_m$ torsion angle closely correlates with and is about one-half the ruffling dihedral angle. The theoretical curves are least-squares fits using the quadratic equation:

$$\nu = \nu_0 + a\varphi^2 \qquad (1)$$

where φ is the torsion in the $C_\alpha-C_m$ bond and ν_0 and a are the parameters that are varied to fit the data by the least-squares method.

The fits using (1) are shown in Figure 7a. The fits are excellent except for the outlier, NiTcPrP (Ni-**11a**). This angular dependence might be expected for these normal modes, which the normal coordinate analyses indicate have sizable contributions from stretching of the $C_\alpha-C_m$ bond. Torsions in this bond

(37) (a) Cullen, D. L.; Meyer, E. F. *J. Am. Chem. Soc.* **1974**, *96*, 2095. (b) Brennan, T. D.; Scheidt, W. R.; Shelnutt, J. A. *J. Am. Chem. Soc.* **1988**, *110*, 3919.

(38) Barkigia, K.; Fajer, J. Personal communication. NiTPrP is planar in the only known crystalline form.

(39) Sparks, L. D.; Anderson, K. K.; Medforth, C. J.; Smith, K. M.; Shelnutt, J. A. *Inorg. Chem.* **1994**, *33*, 2297.

would reasonably lower the stretching force constant because of poorer overlap and decreased conjugation of the p_z orbitals of the C_α and C_m carbons of the macrocycle.

The large width of a number of the Raman lines, including ν_2, ν_3, ν_{28} (or ν_{11}), and possibly ν_8 and other low-frequency lines, can be attributed to conformational heterogeneity in the magnitude of the ruffling. Two types of heterogeneity can contribute. First, a planar conformer can coexist with a nonplanar conformer. The possibility of both planar and nonplanar conformers arises because of the energetic trade-off between enhanced conjugation in the planar macrocycle and optimal Ni−N bond formation in the contracted core of a nonplanar macrocycle. The second type of conformational heterogeneity results from disorder in the orientation of the peripheral substituents. Furthermore, these two types of heterogeneity are interrelated. The larger width of the ν_2 Raman line for NiTEtP, NiTPrP, and NiTPeP in comparison with NiTMeP supports a significant contribution from this substituent−conformer-specific type of heterogeneity for the tetrasubstituted porphyrins. Heterogeneity shows up best in lines like ν_2 because of the large frequency downshift upon ruffling. The large downshift guarantees that the resulting asymmetry and broadening in the line will be large enough to be evident. NiTMeP, for which the calculations do not give multiple conformers differing in the methyl group orientations, has a much narrower ν_2 line suggesting a single ruffled conformer. Molecular mechanics calculations predict that multiple conformers resulting from different substituent group orientations are possible for other tetrasubstituted porphyrins including the linear alkyl, isopropyl, cyclohexyl, and apopinenyl derivatives.[40] This is a consequence of the reduced rotational freedom of the larger substituents.

INDO/s Molecular Orbital Calculations. The INDO/s semiempirical quantum calculations, based on the macrocycle conformations given by the molecular mechanics calculations, accurately predict differences in the transition energies for the Q and B electronic states. This is illustrated in Figure 12, which shows that the predicted and observed trends in the wavelengths of the absorption maxima agree. However, there is a consistent underestimation of the Q-band wavelength and a consistent overestimation of the B-band wavelength. The red shifts in the transitions result from the ruffling of the macrocycle (proportional to the C_α−C_m torsion angle) and not the small differences in the electronic properties of the substituents. This was demonstrated by carrying out INDO calculations on the same macrocycle conformations, but with methyl groups replacing the actual alkyl substituents. These calculations gave nearly the same trends with the C_α−C_m torsion angle as that shown in Figure 12.

The excited state configurations in which one of the electrons of the $a_{1u}(\pi)$ or $a_{2u}(\pi)$ orbitals is promoted to one of the degenerate pair of $e_g(\pi^*)$ orbitals give rise to the Q and B states upon mixing by configuration interaction. Figures S3 and S4 of the supporting information show that the origin of the red shift is a decrease upon ruffling in the separation of the highest filled $a_{1u}(\pi)$ or $a_{2u}(\pi)$ orbitals and the lowest unoccupied $e_g(\pi^*)$ orbitals. The decrease in the separation is primarily a result of a destabilization of the $a_{1u}(\pi)$ and $a_{2u}(\pi)$ orbitals caused by ruffling; the energy of $e_g(\pi^*)$ orbitals by contrast are relatively unchanged by ruffling.

(40) By these arguments NiTtBuP and NiTAdP should have narrow Raman lines because only one conformer is accessible at room temperature. This is generally the case for the high-frequency lines except for ν_2, which we believe to be broadened by an accidental degeneracy with another Raman line at slightly lower frequency than ν_2. This is also true for the structure-sensitive low-frequency region (200−600 cm^{-1}). The lines in the mid-frequency region are substituent modes and should not be considered for this comparison.

The extinction coefficient of the Q band is observed to increase relative to that of the B band. Figure S5 of the supporting information shows a plot of the oscillator strength of the Q and B bands. The oscillator strength of the Q band is seen to be relatively constant; however, the oscillator strength of the B band decreases by 39% as the macrocycle ruffles in the series of Ni tetrasubstituted porphyrins. The decrease in the B-band oscillator strength is consistent with the observed increase in the intensity of the Q band relative to the Soret (Figure 3). The decrease in the B-band oscillator strength is probably due to the decrease in conjugation with increased ruffling of the macrocycle.

The low-lying states involving the metal d orbitals include the d → d* transitions to the empty $d_{x^2-y^2}$ orbital and porphyrin π to $d_{x^2-y^2}$ transitions. As a result of the core contraction that occurs with ruffling the antibonding $d_{x^2-y^2}$ orbital greatly increases in energy relative to the other d orbitals and the $a_{1u}(\pi)$ or $a_{2u}(\pi)$ orbitals. Thus, transitions to $d_{x^2-y^2}$ from filled d_{z^2}, d_π, and d_{xy} orbitals and the $a_{1u}(\pi)$ or $a_{2u}(\pi)$ orbitals give singlet transitions in the region of the Q and B bands and the transition energies move to higher energy as the macrocycle ruffles. The lowest lying $d_{z^2} \rightarrow d_{x^2-y^2}$ transition moves from well below the Q transition to well above, crossing over at a C_α−C_m torsion angle of about 15° as shown in Figure S6 of the supporting information.

The triplet state energies for several porphyrins of the series are plotted in Figure S7 of the supporting information. The INDO/s calculations predict that all of the metal-centered transitions move above the lowest lying triplet π−π^* state ($a_{2u} \rightarrow e_g$) for the most ruffled porphyrins; therefore, NiTAdP and NiTtBuP should phosphoresce unless they decay via a conformer other than the *ruf* conformer. On the other hand, the INDO/s calculations may not accurately predict the relative energies of the metal orbitals relative to the porphyrin orbitals, although the trends in the energies of the transitions should be valid.

Conclusions

The classification of nonplanar distortions of porphyrins according to static deformations along the lowest frequency normal modes of A_{2u} (*dom*), B_{1u} (*ruf*), B_{2u} (*sad*), and E_g (*wav*) symmetry provides a framework for discussion of the relative chemical and photophysical properties of these macrocycle conformers. Structures of symmetrically substituted porphyrins obtained from either molecular modeling calculations or X-ray crystallography generally exhibit nonplanar conformations that can be associated with one or more of these symmetric distortion types.

The nickel tetraalkylporphyrins generally give the *ruf* conformer as the lowest energy conformation in the calculations, and the *ruf* conformer is also generally observed in the crystal structures. The degree of ruffling depends on the steric repulsion between the peripheral substituents and the β-carbons and hydrogens of the pyrrole rings; however, in the crystal, packing forces also act to modify the degree of ruffling and/or impose distortions of other symmetries upon the macrocycle. In addition, most of the tetrasubstituted porphyrins possess stable conformers of the other symmetries at higher energy than the *ruf* conformer. These conformers usually result from differing substituent orientations (α^4, $\alpha^3\beta$, $\alpha^2\beta^2$, $\alpha\beta\alpha\beta$), which act as symmetric perturbations to lower the macrocycle symmetry from D_{4h}. The relative energies of these nonplanar conformers (and the planar conformer) and the barriers to conversion between them depend on the size of the substituents and the size and electronic configuration of the metal incorporated into the porphyrin.

Resonance Raman spectra and absorption spectra of the series of nickel tetrasubstituted porphyrins show that the nonplanarity

of the porphyrin macrocycle increases as the steric bulk of the *meso* substituents increases. The increase in ruffling is evident in the downshifts in the structure-sensitive Raman lines. Furthermore, for small substituents, nonplanar conformers of different types coexist at room temperature, contributing to the conformational heterogeneity evident in the large widths and asymmetric shapes of structure-sensitive Raman lines. For the smallest substituents like the linear alkyls, additional heterogeneity results from the small difference in the energies between the planar conformer and the nonplanar conformers so that all are in equilibrium at room temperature. For very bulky substituents, conformers other than those exhibiting the *ruf* distortion are at much higher energy with large energy barriers between the conformers. Thus, in this case, only the *ruf* conformer is observed and the Raman lines show no evidence of structural heterogeneity. The calculated degree of ruffling correlates both with red shifts in the absorption bands and with downshifts in the frequencies of the Raman marker lines, incidentally indicating that the molecular mechanics calculations are accurate enough to be useful.

Comparisons between X-ray crystal structures and calculated structures generally show good agreement; however, some systematic differences are found. The ability of the INDO/s calculations based on the molecular structures obtained from molecular mechanics to quantitatively reproduce the red shifts in the absorption bands also support the general accuracy of the calculations and, further, point to ruffling as the origin of the band shifts.

It is important to find a spectroscopic means of distinguishing the B_{1u} distortion from other nonplanar distortions, but as yet, no characteristic spectroscopic features allow us to distinguish between the different conformers. This is a primary goal for future studies of nonplanar porphyrins and their conformers.

The tetrasubstituted porphyrins provide a useful model system for investigation of the changes in chemical properties brought about by the ruffling distortion of the heme in cytochrome *c*. The moderate degree of distortion of the heme in cytochrome *c* is roughly equivalent to that occurring for some conformers of NiTEtP. Energetically, the ruffling of the heme may be more significant however because ruffling is more difficult for the Fe(II) and Fe(III) ions which are larger than Ni(II).

The foregoing results and conclusions have important implications for understanding the role of nonplanar distortions in the biological function of proteins like cytochrome *c* that contain nonplanar porphyrins. The primary question to be addressed for cytochrome *c* is what influence ruffling has on the properties of the heme and how changes in these properties influence electron-transfer reactions. Clearly, INDO/s calculations, as already noted by others,[6a] suggest that the reduction potentials of the ring and metal are influenced by ruffling. Thus, the protein environment of the porphyrins in proteins can influence the redox properties, and thus electron-transfer reactions, by controlling the nonplanarity of the macrocycle. In addition, the protein can also influence the relative energies of various conformers as, for example, in cytochrome *c*, where the *ruf* conformer is stabilized over the planar, *wav*, *sad*, and *dom* conformers. Further, changes in metal size clearly affect the relative energies of the planar and the nonplanar conformers; therefore, the oxidation state of the Fe atom can influence protein structure through the energetics of the nonplanar conformers and their interaction with the surrounding protein. Thus, changes in the relative energies of the conformers may influence the equilibrium structure of the apoprotein moiety and ultimately protein−protein binding events during electron transport.

A ruffled porphyrin macrocycle can also impart unique chemical reactivities to the porphyrin. In fact, novel reactivity at the *meso* position of the macrocycle has been reported for tetra-*tert*-butylporphyrin.[14] The position and orientation of chiral substituents, as in the case of TMyP and the TcPrP derivative **11a**, can also be used to control steric interactions with prochiral substrate molecules to give enantiomeric selectivity in catalytic reactions.[18] In the latter case, different reactivities would be expected for the same porphyrin in another nonplanar distortion type because the steric properties would differ between the conformers.

Finally, the photophysical properties of related pigments in photosynthetic reaction centers could be influenced by photo-induced interconversion between conformers. For example, conformational gating of electron-transfer reactions in the reaction centers may play a role in the initial events of photosynthesis. This has been suggested previously for electronic-induced structural changes in the primary donor.[41] Also, the protein moiety of reaction centers may control electron-transfer rates by stabilizing certain conformers over others.

Acknowledgment. We thank Drs. Jack Fajer and Cathy Barkigia for a sample of nickel tetrapropylporphyrin, for communicating their X-ray diffraction results, and for helpful discussions. Work at Sandia National Laboratories supported by U.S. DOE Contract DE-AC04-94AL85000 and Associated Western Universities Fellowships (W.J., J.D.H., X.S.) and other support from a DOE Distinguished Postdoctoral Fellowship (M.C.S.), the Centre National de la Recherche Scientifique (CNRS, Grant URA 1194) (J.C.M.), a National Science Foundation Grant (CHE-93-05577) (K.M.S.), and a DOE-AICD Grant (W.A.G.) are acknowledged.

Supporting Information Available: Table S1 giving the parameters of the force field used in the molecular mechanics calculations, Figure S1 showing the powder resonance Raman spectra of selected nickel porphyrins of the series, Figure S2 showing the space-filling model of the conformers of NiTEtP also shown in Figure 9 and the space-filling models of the porphyrin also shown in Figure 8, Figure S3 plotting the energies of the HOMO and LUMO π orbitals as a function of the $C_\alpha-C_m$ torsion angle in the energy-optimized molecular mechanics structure, Figure S4 plotting the LUMO−HOMO energy separation ($e_g - {}^1/_2[a_{2u} + a_{1u}]$) as a function of the $C_\alpha-C_m$ torsion angle, Figure S5 plotting the Q- and B-band oscillator strengths as a function of the $C_\alpha-C_m$ torsion angle, Figure S6 plotting the energies of the singlet Q and B transitions and the $d \rightarrow d^*$ and $a_{1u} \rightarrow d^*$ transitions as a function of the $C_\alpha-C_m$ torsion angle, and Figure S7 showing the transitions energies of the triplet states as a function of the $C_\alpha-C_m$ torsion angle (14 pages). This material is contained in many libraries on microfiche, immediately follows this article in the microfilm version of the journal, can be ordered from the ACS, and can be downloaded from the Internet; see any current masthead page for ordering information and Internet access instructions.

JA9510727

(41) Renner, M. W.; Barkigia, K. M.; Zhang, Y.; Medforth, C. J.; Smith, K. M.; Fajer, J. *J. Am. Chem. Soc.* **1994**, *116*, 8582.